A Thesis for the Degree of Master of Science

Hirsutenone suppresses adipogenesis in 3T3-L1 preadipocytes by targeting PI3K and ERK

PI3K 와 ERK 의 활성 저해를 통한 허수테논의 3T3-L1 지방세포형성 억제 효능

By

Lai Yee Cheong

Department of Agricultural Biotechnology

Seoul National University

August, 2013

Abstract

The growing prevalence of obesity and overweight has become a global health problem. Many potential natural products act as alternatives for the prevention and/or treatment of obesity due to the side effects of obesity-treatment drugs. In the present study, the anti-adipogenic effect of hirsutenone, a diarylheptanoid compound from *Alnus japonica* and *Alnus hirsuta* has been investigated using 3T3-L1 preadipocytes. Hirsutenone concentration-dependently suppressed adipogenic cocktail-induced lipid accumulation during adipogenesis, which is associated with decreased protein expression levels of peroxisome proliferator-activated receptor-γ (PPARγ), CCAT/enhancer-binding protein-α (C/EBPα) and fatty acid synthase (FAS). This inhibitory effect was largely due to the early stage of adipogenesis through mitotic clonal expansion (MCE), evidenced by delayed cell cycle entry of preadipocytes to S phase from G1 phase after 20 hours of initiation of adipogenesis. Furthermore, hirsutenone suppressed MCE was accompanied by reduced-

activation of Akt/protein kinase B (PKB) signaling pathway and suppressed phosphorylation level of p90RSK without altering the upstream of ERK signaling pathway. Hirsutenone was shown to bind directly to phosphatidylinositol 3-kinase (PI3K) and extracellular-related kinase 1 (ERK1), which subsequently inhibited both kinases activity. Taken together, these results demonstrate that hirsutenone modulates MCE by directly targeting PI3K and ERK1 to suppress their activities in the early phase of adipocyte differentiation.

Keywords: Hirsutenone; adipogenesis; mitotic clonal expansion; PI3K; ERK; 3T3-L1 preadipocytes

Student ID: 2011-24270

Contents

I. Introduction

Obesity has become epidemic and is the fifth leading risk for global deaths with more than 1.4 billion overweight persons aged 20 years and above, at least 500 million of them are obese due to a sedentary lifestyle and diets richer in caloric and fat [1]. Even in most of the Asian countries the prevalence of overweight and obesity has increased many folds in the past few decades though magnitude varies among countries [2].

Obesity is characterized by energy imbalance and leads to storage of excess energy as triglyceride in adipocytes. As adipocytes continue in storing lipids, they can exhibit hypertrophy (increased cell size) and hyperplasia (increased cell number) [3, 4] as adipose tissue has a remarkable capacity to remodel and adapt to the nutritional environment in the body. Adipocytes are not only playing a role as reservoir in storing and releasing fuel, but also as endocrine cells in secreting factors that regulate whole-body energy metabolism [3, 5]. Therefore the process of adipose hypertrophy

and hyperplasia are accompanied with intracellular abnormalities of adipocyte function [6] which contribute to metabolic diseases in obesity including type 2 diabetes, insulin resistance, hypertension, coronary heart disease, stroke, cancer and others [1].

Adipose tissue is able to regenerate fat cells by *de novo* adipogenesis from adipocyte precursor cells, which then proliferate and re-differentiate into mature adipocytes [7]. Adipogenesis is a process of cell differentiation from preadipocytes to adipocytes which can be divided into growth arrest, mitotic clonal expansion (MCE) and terminal differentiation [8-10]. Especially MCE is a prerequisite step for terminal differentiation [11-13] where growth-arrested cells synchronously re-enter cell cycle leads to cell numbers are increased. Therefore controlling adipogenesis and energy homeostasis are thought to be a critical part to combat obesity [14].

One widely used *in vitro* model for studying the adipocyte is 3T3-L1 cell line, which is derived from disaggregated mouse

embryos and has proven to be a faithful model for studying adipocyte biology, especially in adipogenesis and energy metabolism [3]. In order to induce the adipogenic differentiation program of 3T3-L1 preadipocytes, addition of glucocorticoids, cAMP enhancer and insulin is required to initiate a transcriptional regulatory cascade that results in a gene expression profile specific for adipocyte functions [15]. These changes are regulated by several transcription factors such as CCAT/enhancer-binding proteins (C/EBPs), peroxisome proliferator-activated receptor-γ (PPARγ), adipocyte determination and differentiation factor 1 /sterol regulatory element binding protein ADD1/SREBP1c and fatty acid synthase (FAS) [9] to conduct adipogenesis and lipogenesis [16]. Among those mixture of hormone cocktail, insulin has a remarkable influence on adipogenesis in vivo and in vitro [17] by promoting preadipocyte differentiation and enhancing lipid accumulation in adipocytes. Insulin signaling in the early differentiation involves the activation of the insulin receptor tyrosine kinase followed by the activation of phosphoinositide 3 -

kinase (PI3K) / protein kinase B (AKT) pathway and the Ras-mitogen-activated protein kinase (MAPK) pathway [18, 19]. MAPK and Akt signaling pathways are involved in MCE to mediate proliferation signals during early phase of adipogenesis [11, 20, 21]. In addition, inhibition of PI3K could impair adipogenesis [22, 23]. All these studies are suggesting that suppression of the early stage of adipogenesis, including MCE can prevent adipocyte differentiation and consequently lead to anti-obesity effect.

There are quite a number of medications which are available for the treatment of obesity, however have minimal efficacy and poor side-effect profiles [24, 25]. Therefore it is important to search for prevention or treatment of obesity with better efficacy and less side-effect. In recent decades, there is an increasing interest in identifying naturally occurring phytochemicals capable of preventing obesity because natural extracts from plants represent the oldest and most widespread form of pharmaceutical treatment [16, 26].

According to Korea Food and Drug Administration (KFDA), fifteen *Alnus* species are indigenous in Korea. The members of genus *Alnus* are well known for their traditional medicinal values which as remedies for fever, hemorrhage, diarrhea, lymphatic disease, alcoholism, cancers and diabetes [27-29]. Alder contains variety of bioactive constituents, among them, diarylheptanoids are the dominant group [30]. Recently, there was a study related to anti-adipogenic diarylheptanoids from *Alnus hirsuta* f. *sibrica* on 3T3-L1 cells model by suppressing the induction of PPARγ and C/EBPα [31]. Hirsutenone (HST) (Figure 1A) is an active form of diarylheptanoid compound can be isolated from *Alnus japonica* [30, 32] and *Alnus hirsuta* [30]. Previous studies have shown that HST has a wide range of biological activities, including anti-inflammatory, anti-tumor promoting and anti-atopic dermatitis effects [33-36]. However, to date, the molecular mechanisms underlying the anti-adipogenic properties of HST remain unknown and further investigation is required. Therefore the present study was designed to investigate on (1) how HST exerts anti-adipogenic

activity at different stages of adipogenesis and (2) its related molecular mechanism in inhibition of adipocyte differentiation using 3T3-L1 preadipocytes.

II. MATERIALS AND METHODS

2.1 Materials

Synthesis of natural compound Hirsutenone (HST) from curcumin was carried out by Dr. Thimmegowda. As a brief description, hydrogenation of 1,6- diene double bonds of curcumin with 10% pelladium on carbon catalyst using parr hydrogenation apparatus afforded *1,7-bis(4-hydroxy-3-methoxyphenyl)heptane-3,5-dione* in 59% yield and also the double bond and single carbonyl group reduced compound 5-hydroxy-1, 7-bis (4-hydroxy-3-methoxyphenyl) heptan-3-one in 25 % yield. Reduction of carbonyl group of 1,*7-bis(4-hydroxy-3-methoxyphenyl) heptane-3,5-dione* using sodium borohydride gave the single carbonyl group reduced compound 5-hydroxy-1, 7-bis (4-hydroxy-3-methoxyphenyl) heptan-3-one in 25 % yield. Dehydration of 5-hydroxy-1, 7-bis (4-hydroxy-3-methoxyphenyl) heptan-3-one using catalytic amount of *P*-Toluenesulfonic acid gave (*E*) - 1, 7-bis(4-hydroxy-3-methoxyphenyl) hept-4-en-3-one (Gingerenone A) in 77% yield.

Demethylation of (*E*) - 1, 7-bis(4-hydroxy-3-methoxyphenyl)hept-4-en-3-one (Gingerenone A) using $AlCl_3$/Pyridine afforded the desired compound HST [(*E*)-1,7-bis(3,4-dihydroxyphenyl)hept-4-en-3-one] in 20% yield.

Dulbecco-modified Eagle medium (DMEM) and fetal bovine serum (FBS) were purchased from WELGENE, INC. (Daegu, South Korea). Bovine Calf Serum (BCS) were purchased from GIBCO (Grand Island, NY). Methylisobutylxantine (IBMX), dexamethasone, human insulin 10 mg/mL, Oil Red O powder were purchased from Sigam (St. Louis, MO). 3-[4,5-diethylthiazol-2-yl]-2,5-diphenyltetrazolium bromide (MTT) was purchased from USB (Cleveland, OH, USA). Isopropyl alcohol was obtained from Amresco LLC (Amresco, Solon, OH). Antibody against PPAR gamma, total ERK and phospho-ERK were purchased from Santa Cruz Biotechnology, Inc (Santa Cruz, CA). Antibody against FAS, total Akt, phosphor-Akt,, RSK1/2/3, phosho-p90RSK, phospho-p70S6K and p70S6K were obtained from Cell Signaling Biotechnology (Beverly, MA). Antibody against β-actin was

purchased from Sigma Chemical (St. Louis, MO).

2.2 Cell culture and preadipocytes differentiation

3T3-L1 preadipocytes were purchased from ATCC (Manassas, VA). Media and serum were obtained from WELGENE, INC. (Daegu, South Korea) and GIBCO (Grand Island, NY), respectively. 3T3-L1 preadipocytes were maintained in Dulbecco's modified Eagle's medium (DMEM) supplemented with 10 % bovine calf serum (BCS), at 10 % CO_2 and 37°C until 100 % confluence. After 2 days of post-confluent (day 0), cells were incubated in DMEM supplemented with 10 % fetal bovine serum (FBS) and adipogenic cocktail (MDI) which was a mixture of 0.5 mM 3-isobutyl-1-methylxanthine (IBMX), 1 μM dexamethasone (DEX) and 5 μg/mL insulin for 2 days in order to induce differentiation. After 2 days, medium was changed to DMEM containing 10 % FBS and 5 μg/mL insulin. Two days later, cells were switched to maintenance medium containing DMEM and 10 % FBS until preadipocytes were fully differentiated. The maintenance

medium was changed every 2 days.

2.3 3-[4,5-diethylthiazol-2-yl]-2,5-diphenyltetrazolium bromide (MTT) assay

Cell viability was evaluated by MTT (3-[4,5-diethylthiazol-2-yl]-2,5-diphenyltetrazolium bromide) assay, which measures the mitochondrial reduction of MTT to formazan. 3T3-L1 preadipocytes were seeded in 96-well plate at a density of 5.0×10^4 cells per well. After confluence, one group of cells were treated with MDI cocktail as a control and the rest were treated with MDI contained 20, 40, 80 and 100 μM of HST for 2 days. Subsequent incubation of the cells with MTT solution (0.5 mg/mL) for 1 hour at 37°C to allow formation of violet crystals (formazan). Crystal form of formazan was dissolved in DMSO and the absorbance was measured at 595 nm with a microplate reader (Beckman-Coulter, CA).

2.4 Lactate dehydrogenase (LDH) assay

Cytotoxicity was assessed with an LDH (lactate dehydrogenase)-cytotoxicity detection kit (Takara Bio Inc.) which allows measurement of LDH activity released from the damaged cells into the supernatant. This enzyme can be detected by measuring its catalytic activity and indirectly the conversion of 2-(4-Iodophenyl)-3-(4-nitrophenyl)-5-phenyl-2H-tetrazolium chloride (INT) to another water-soluble formazan dye. Experiment was carried out according to the manufacturer's protocol. Briefly, 3T3-L1 preadipocytes were seeded in 96-well plate at a density of 5.0 x 10^4 cells per well. After confluence, one group of cells were treated with MDI cocktail as a control and the rest were treated with MDI contained 20, 40, 80 and 100 µM of HST respectively for 2days. 50 µl of supernatant per well was harvested and transferred into a new 96-well, flat-bottom plate. Reaction mixture (50 µl) was added to each well and incubated for 15 minutes at room temperature (RT) protected from light. The absorbance of the samples was measure at 490 nm with an ELISA reader.

Cytotoxicity was calculated with the formula: % cytotoxicity = (experimental value – low control) x 100 / (high control – low control), where low control is assay medium with cells and high control is assay medium (plus 2% Triton X-1) with cells.

2.5 Oil Red O staining

3T3-L1 preadipocytes were seeded in 24-well plate at a density of 5.0 x 10^4 cells per well. After confluence, the cells were incubated as described above in the cell culture section 2.2 in order to perform cell differentiation. On day 6, differentiated cells were subjected to Oil Red O staining to visualize accumulated lipid droplets in the cells. Media were removed and differentiated cells were fixed with 10 % formalin for 20 min followed by phosphate buffered saline (PBS) washing. The fixed cells were then stained with Oil Red O solution for 15 min. Oil Red O solution was prepared by dissolving 0.25 mg Oil Red O powder in 50 mL 60 % isopropyl alcohol followed by filtering with 0.45 µm membrane

(Whatman, Piscataway, NJ). After staining, the cells were washed thrice with PBS. Intracellular lipid content was quantified by eluting Oil Red O stain with isopropyl alcohol and measured at 515 nm with spectrophotometry.

2.6 Western blot assay

3T3-L1 preadipocytes were cultured in DMEM supplemented with 10 % BCS, at 10 % CO_2 and 37°C until 100 % confluence. The medium was changed to DMEM supplemented with 10 % FBS and MDI adipogenic cocktail with or without HST at indicated concentrations. Cells were harvested by scraping in cell lysis buffer and the protein concentration of each sample was determined by using a dye-binding protein assay kit (Bio-Rad Laboratories, Hercules, CA) according to the manufacturer's instruction. Cell lysates were subjected to sodium dodecyl sulfate-polyacrylamide gel electrophoresis (SDS-PAGE) and transferred to a 0.2 μm nitrocellulose (NC) transfer membrane (GE healthcare,

Whatman). The membrane was blocked with 5 % skim milk for an hour at room temperature followed by specific primary antibody incubation at 4°C overnight. HRP-conjugated secondary antibody was incubated with membrane following primary antibody incubation. In between every step, membrane was washed with a mixture of Tris-Buffered Saline and 0.1 % Tween 20 (TBS-T) solution. The protein bands were visualized using a chemiluminescence detection kit (Amersham Pharmacia Biotech, Piscataway, NJ).

2.7 Trypan blue assay

3T3-L1 preadipocytes were seeded in 6-well plates at a density of 5 x 10^4 cells per well, and incubated in DMEM supplemented with 10 % FBS and MDI cocktail in the presence or absence of 80 μM HST. After that, cells were trypsinized and stained with 0.4 % of Trypan blue by incubating at room temperature for 5 minutes. The stained cells were loaded onto a

hematocytometer, and the viable cells were counted.

2.8 Flow cytometry using a fluorescence-activated cell sorter (FACS)

3T3-L1 preadipocytes (10 x 10^4 cells per dish) were seeded in 6 cm dish and cultured until confluence. After 2 days of post-confluent cells were incubated in DMEM supplemented with 10% fetal bovine serum (FBS) and adipogenic cocktail (1 µM dexamethasone, 0.5 mM 3-isobutyl-1-methylxanthine (IBMX), 5 µg/ml insulin) and with and without 80 µM HST for 0 hour, 16 hours, 20 hours, 24 hours, 36 hours and 48 hours respectively. After the incubation time, cells were dissociated by trypsin and centrifuged at 1000 rpm for 3 min. The pellets were resuspended in PBS and centrifuged at 1000 rpm for 3 min again for washing purpose. The pellets were suspended in cold 70 % (v/v) ethanol for fixing and maintained at 4°C overnight. Then cells were centrifuged at 1500 rpm for 3 min and resuspended in 600 µl of

PBS containing 20 μg/ml of propidium iodide solution (PI) (Sigma) and 0.2 mg/ml of RNase (Sigma). Next, cells were incubated at 37°C for 15 min in the dark. Finally, fluorescence emitted from cells was measured with a flow cytometer (Becton-Dickson, San Jose, CA, USA). A total of ten thousand cells in each sample were analyzed.

2.9 PI3K kinase assay

Active PI3K protein (100 ng) was incubated with 20 μM, 40 μM and 80 μM of HST or 20 μM LY294002, PI3K inhibitor, for 10 minutes at 30°C. After that 20 μL of 0.5 mg/mL phosphatidylinositol (Avanti Polar Lipids, Alabaster, AL) was added and incubated for 5 minutes at room temperature. Then reaction buffer (100 mM HEPES [pH 7.6], 50 mM $MgCl_2$ and 250 μM ATP) containing 10 μCi of [γ-^{32}P] ATP was added and incubated for 10 minutes at 30°C. The reaction was stopped by adding 15 μL of 4 N HCl and 130 μL of a chloroform and methanol mixture (1:1).

After vortexing, 30 µL of the lower chloroform phase was spotted onto 1 hour pre-activated at 110 °C of 1 % potassium oxalate-coated silica gel plates. The spotted chloroform phase was separated through thin-layer chromatography and radio-labeled spots were visualized by autoradiography.

3.0 ERK kinase assay

In brief, each reaction contained 5 x reaction buffer [125 mM Tris/HCl pH 7.5 and 0.1 mM EGTA], active MAP kinase 1 [50 mM Tris/HCl pH 7.5, 0.1 mM EGTA, 0.1 mM sodium orthovanadate ($Na_3VO_{4)}$, 0.1 % 2-mercaptoethanol and 1 mg/mL BSA], along with magnesium acetate (MgAc)-ATP cocktail buffer [25 mM MgAc and 0.25 mM ATP]. Active ERK1 protein (10 ng) or ERK2 protein (100 ng) was incubated with presence or absence of 20, 40 and 80 µM of HST for 10 minutes at 30°C. After that, 0.33 mM of Myelin Basic Protein (MBP) substrate was added followed by 10 µL of diluted [γ-32P]ATP solution and incubated at

30°C for 10 minutes with the above assay buffer and substrate peptide. Then 26 μL aliquots were transferred onto p81 filter paper and washed 3 times with 0.75 % phosphoric acid for 5 minutes per wash, followed by washing once with acetone for 5 minutes. The incorporation of radioactivity was determined by scintillation counter.

3.1 Pull-down assay

Sepharose 4B freeze-dried powder (0.3 g; GE Healthcare) was activated in 1 mM HCl and suspended in HST (2 mg) coupled solution (0.1 M $NaHCO_3$ and 0.5 M NaCl). Following overnight rotation at 4°C, the mixture was transferred to 0.1 M Tris-HCl buffer (pH 8.0) and again further rotated at 4°C overnight. The mixture was washed three times with 0.1 M acetate buffer (pH 4.0) and 0.1 M Tris-HCl + 0.5 M NaCl buffer (pH 8.0), respectively, and suspended in PBS. The pull down assay was performed as previously described [37]. Briefly, active protein (ERK1 or PI3K) was incubated with Sepharose 4B alone or HST-Sepharose 4B

beads in reaction buffer. After incubation at 4°C, the beads were washed in washing buffer and proteins bound to the beads were analyzed by immunoblotting.

3.2 ATP and HST competition assay

0.2 µg active protein (ERK1) was incubated with 100 µl of HST-Sepharose 4B or control Sepharose 4B beads in the presence or absence of 10 or 100 µM of adenosine triphosphate (ATP) in the reaction buffer. The protein was pulled down and analyzed by immunoblotting following overnight incubation at 4°C.

3.3 Statistical analysis

Data are expressed as means ± standard deviation (S.D) values and each group were compared by Student's *t* test where $p < 0.05$, 0.01 and 0.001 were considered significant.

III. Results

3.1 HST inhibits MDI-induced adipogenesis in 3T3-L1 preadipocytes

Firstly, the effect of HST on the differentiation of 3T3-L1 preadipocytes to adipocytes was investigated. After 2 days post-confluence, 3T3-L1 preadipocytes were induced to differentiate with and without the presence of HST. As shown in morphologic analysis (Figure 1B), HST decreased lipid accumulation in a concentration-dependent manner at concentrations of 20, 40 and 80 μM where the red staining indicated intracellular lipid droplets. The lipid content was then quantified by Oil Red O staining and the greatest reduction of lipid content was observed at 80 μM of HST, which was approximately 55% reduction (Figure 1C).

Consistent with these results, HST inhibited protein expression levels of PPARγ, C/EBPα and FAS in concentration-dependent manner (Figure 1D). PPARγ and C/EBPα are known as a master transcription factors in adipocyte differentiation [17]. To test

whether this anti-adipogenic effect was resulted from its cytotoxicity, the effect of HST on cell viability of differentiating preadipocytes was performed by MTT and LDH assays. Cells were treated with different concentrations (0, 20, 40, 80, 100 μM) of HST for 48 hours. As shown in Figure 1E, treatment of HST (20 – 100 μM) showed no effect on cell viability but with a 12% increment in cytotoxicity at 100 μM. Therefore, HST (20, 40 and 80 μM) inhibits adipogenesis in 3T3-L1 preadipocytes without affecting cell viability and cytotoxicity.

3.2 HST mainly suppresses early stage of 3T3-L1 preadipocytes differentiation

To further understand HST in inhibiting related adipogenesis mechanism in 3T3-L1 cells, the most sensitive adipogenesis stage to the function of HST has to be identified. Adipogenesis process can be divided into early stage (days 0-2), intermediate stage (days 2-4) and late stage (days 4-6). As shown in Figure 2A, 80 μM of

HST was given to the differentiating cells at the indicated times of adipogenesis. Visualization of lipid accumulation by Oil Red O staining is shown in Figure 2B. Cells were subjected to a quantification of Oil Red O staining of intracellular lipids after 6 days of fully differentiation. Consistent with the result shown in Figure 1D, cells treated with HST from 0-6 days also showed a reduced of 60 % lipid content. Interestingly, there was a significantly decrease by 43% in adipogenesis only for the first 2 days of HST treatment (Figure 2C). Based on Figure 2C, the differentiating cells treated with HST have showed a greater lipid reduction than the other groups when the first 2 days was included in the treatment period.

However, differentiating cells treated with HST only during intermediate stage (including days 2-4) and late stage (including days 4-6) exhibited a 21% and 7% decrease, respectively. In addition, the cells in treatment period from day 2 to day 6 showed ~27% reduce in lipid accumulation as compared with the

differentiated control. Besides that, during the intermediate stage treatment, HST treatment displayed significantly reduced-levels of lipid content compared with differentiated control cells, suggesting that HST may has an additional role in modulating lipogenesis during intermediate and later stage of differentiation. Collectively, all these results indicate that the anti-adipogenesis effect of HST is primarily contributed to the early stage of differentiation.

3.3 HST delays MDI-induced MCE in the early stage of adipogenesis

To further assess the effect of HST in the early stage which involves MCE, cell proliferation and cell cycle progression were evaluated. As expected, total cell numbers were increased in MDI treatment group over 24 and 48 hours, while HST significantly suppressed the increase of cell numbers (Figure 3A). In order to find out whether it was associated with cell cycle arrest during MCE, flow cytometry assay was performed. Based on the

results (Figure 3B and C), MDI-induced cell cycle entry of differentiating preadipocytes to G2/M phase in 24 hours which are consistent with previous results [38, 39]. During the presence of 80 μM of HST, it induced a suppression of cell cycle entry to S and G2/M phases at both 20 and 24 hours, respectively. As shown in Figure 3C, the majority of cells (65 % of total cells) in 80 μM of HST-treated group were retained in G1 phase when compared with only MDI-induced group at 20 hour. At 24 hour, more cells were retained in G1 phase (53 % of total cells) if compared with MDI-induced group which contained the majority of cells (56 % of total cells) in G2/M phase. However, further incubation of differentiating preadipocytes with HST to 36 and 48 hours resulted in the cell cycle entry to S and G2/M phases respectively if compared with only MDI-induced group (Figure 3B). These results implicate that HST exhibits anti-adipogenesis effect by delaying cell cycle progression at 20 and 24-hour during early stage of differentiation.

3.4 HST regulates MDI-induced Akt- and ERK-mediated signaling pathways in the early phase of adipogenesis

The altered expression of transcriptional factors and cell cycle arrest led to speculate about its potential impairing effects on PI3K/AKT and ERK signaling pathway which are known to regulate cell proliferation [11]. As expected, treatment of HST (20, 40 and 80 μM) markedly downregulated MDI-induced phosphorylation of AKT in concentration-dependent manner as well as its downstream signaling protein, p70S6K (Figure 4A).

Besides that, ERK-mediated signaling pathway was observed as it also involves in cell proliferation during early stage of adipogenesis [40]. Interestingly, the treatment of HST could not reduce the phosphorylation expression levels of ERK (Figure 4B). However, it is effectively suppressed MDI-induced phosphorylation of p90RSK, a downstream protein of ERK-mediated signaling pathway, in a concentration-dependent manner. All these results demonstrated that HST inhibits MDI-induced cell proliferation by regulating Akt signaling pathway and p90RSK phosphorylation.

3.5 HST suppresses ERK1 kinase activity by binding with ERK1 in an ATP -noncompetitive manner

According to the previous studies, ERK1 isoform, but not ERK2, mainly involves in the regulation of adipocyte differentiation, adiposity and high-fat diet-induced obesity [41, 42]. Therefore, *in vitro* ERK1 activity was measured using kinase assay in order to evaluate the alteration of phosphorylation of p90RSK. As shown in Figure 5A, HST (20, 40 and 80 μM) was significantly suppressed ERK 1 activity in a concentration-dependent manner. This suppression was exerted through direct binding of ERK1 to HST-Sepharose 4B beads in an ATP-noncompetitive manner (Figure 5B and Figure 5C). These results indicate that HST and ATP could interact with ERK1 at different binding sites.

3.6 HST binds with PI3 kinase to inhibit its activity and subsequent downstream signaling cascades during adipogenesis of 3T3-L1 preadipocytes

To investigate whether suppression of Akt phosphorylation was due to the regulation of PI3K activity, *in vitro* PI3 kinase assay was performed (Figure 6A). The suppression effect of HST on PI3K activity was first noted at 20 μM and complete inhibition effect was observed at 40 and 80 μM of HST treatment. These three concentrations of HST exhibited greater extent of inhibition of kinase activity than 20 μM LY294002, a PI3K inhibitor. To further evaluate the interaction between HST and PI3K, a pull down assay was performed, which the result shown that PI3K was precipitated with HST-conjugated Sepharose 4B beads (Figure 6B). This indicates that inhibition activity of downstream signaling cascades results from the direct binding interaction between HST and PI3K.

IV DISCUSSION

Although HST has been suggested to have anti-adipogenic property [31], the underlying molecular mechanism in anti-adipogenesis is still remain unclear. In this study, non-toxic levels of HST exerts an anti-adipogenic property in a concentration-dependent manner and it is largely limited to the early stage of adipogenesis by modulating MCE in cell cycle progression through inhibition of PI3K and ERK activity.

The early stage of inhibitory adipogenesis effect is reflected by the reduction of lipid accumulation content after treating with HST in different treatment periods. Particularly the present evidence clearly indicating that the presence of HST in the first 48 hours of adipogenesis is largely required to inhibit adipogenesis by modulating MCE and insulin signaling pathway. These 2 cellular events occur in the early phase of adipogenesis. The results indicate that HST delays the cell cycle progression from entering S and G2/M phases at 20 and 24 hours respectively after initiation of

adipogenesis with no effect on cell viability. In order to have a better understanding of the function of HST in suppression of MCE, it is suggested to identify target cell cycle regulators such as p27/kip1 and cdk2 [11, 38]. However, whether MCE is an imperative early step for differentiation initiation still remains controversial [11, 21, 43, 44]. Several studies have been done where modulation of MCE could inhibit adipogenesis in 3T3-L1 cells model [38, 39, 45-47].

Growth arrest 3T3-L1 preadipocytes can be differentiate synchronously upon treatment of adipogenic cocktail which is a combination of insulin, a glucocorticoid, a cAMP phosphodiesterase inhibitor to stimulate intracellular cAMP levels and fetal bovine serum [48]. Among these three inducers, insulin appears to be of special importance as it has a potential influence of *in vivo* hyperinsulinemia on the development of obesity and through activation of both PI3 kinase and the prenylation pathways to promote adipogenesis [49]. Although insulin has been known to

induce lipogenesis and glucose uptake in mature adipocytes, undeniable, insulin-induced Akt and ERK signalings are also required for cell cycle progression of preadipocytes in adipogenesis as demonstrated in insulin receptor (IR)-deficient mice [50, 51]. The activities of p70S6K and ERK are regulated in a cell cycle-dependent manner especially at the G0/G1 boundary and cell progressing from M into G1 phase [52]. Therefore the effect of HST on IR-dependent PI3K/Akt pathway in the early phase of adipogenesis has been investigated in this study. However, there was no inhibitory effect of tyrosine phosphorylation site of insulin receptor in HST-treated cells (Data not shown). Nevertheless, HST could downregulate Akt phosphorylation level (Figure 4A) and PI3K activity *in vitro* (Figure 6A). It is supported from the previous studies that disruption of Akt and PI3K can reduce the differentiation of preadipocytes into adipocytes [17, 22, 53-55]. On the other hands, the ability of insulin to activate p90RSK has shown to require MAP kinase (ERK) for differentiation of 3T3-L1 fibroblasts to occur [56]. It is corresponding with the result at

Figure 4B and 5A which HST could inhibit the expression level of p-p90RSK through the suppression of ERK1 activity. Furthermore, this study has identified that ERK1 and PI3K are novel targets for the anti-adipogenic effect of HST (Figure 5B and Figure 6B). HST directly binds ERK1 in an ATP-noncompetitive manner (Figure 5C). This indicates that HST and ATP could interact with ERK1 at different binding sites. Therefore further studies are required to find out the actual binding pocket between HST and ERK1 crystal structures in its active confirmation through molecular modeling system. Further study of ATP competitive assay between HST and PI3K is also necessary to determine their binding interaction.

Those earliest events are followed by the transcription factors of PPARγ and C/EBPα, which are master regulator of adipocyte differentiation and lead to transactivation of adipocyte-specific genes such as fatty acid synthase (FAS) when lipogenesis is promoted to maintain the adipocyte phenotype [9]. FAS is a

lipogenic enzyme that involves in the synthesis and storage of triglycerides [57]. In the present study, HST was able to reduce PPARγ and C/EBPα protein levels as well as FAS expression level in a concentration-dependent manner (Figure 1D). This result is corresponding with the lipid accumulation in adipocytes with or without HST treatment for indicated periods (Figure 2C). There was a significantly reduced level of lipid content during intermediate stage of differentiation. These results indicated that inhibitory effect of HST in adipogenesis may have an additional effect in regulating lipogenesis. Previous study has reported that adipocyte differentiation is blocked after treating with fatty acid synthase inhibitor, C75 [58].

PI3K/Akt signaling pathway involves in a diverse array of biological processes by phosphorylating and regulating a large number of substrates. Even though insulin signaling pathway involves in the early phase of cell differentiation by modulating cell cycle progression, ameliorate this pathway could lead to insulin

resistance [59-61]. Besides adipose, other insulin sensitive tissues and organs, such as liver, muscle and hypothalamus also involves in the inter-tissue communication in the regulation of insulin action. Therefore, tissue-specific differences in the activation of the PI3K/Akt pathway and impact on insulin sensitivity may be different. In a previous study, genetic disruption of the p85α regulatory subunit of PI3K increases hepatic and peripheral insulin sensitivity despite PI3K enzymatic activity is diminished in liver [62]. In addition, a herb formula extract which composed of *Alnus hirsuta* bark has a strong anti-diabetic potential effect has been revealed [28]. Therefore, HST might possibly contribute to attenuate adipogenesis without triggering insulin resistance. However, further studies are necessary to examine the effect of HST in insulin sensitivity and anti-obesity in *in vivo* model.

HST is an active form of diarylheptanoid compound available in the members of genus *Alnus* such *Alnus japonica* and *Alnus hirsuta* [30]. HST is getting to gain attention from scientists

due to its potential medical values such as anti-inflammatory, anti-tumor promoting, anti-atopic dermatitis as well as anti-obesity. However, there is still lack of information about HST such as its percentage composition in alders and bioavailability for the sake of human consumption. This information might play a major role in future research.

In conclusion, a new role of HST in adipogenesis has been discovered through primarily targeting the early phase of differentiation which involves MCE by direct targeting PI3K and ERK1 resulting in suppression of PPARγ and C/EBPα. Therefore, HST might be a useful alternative phytochemical in preventing obesity and obesity-related metabolic disease.

Ⅴ. References

1. Organization, W.H., *Obesity and Overweight, Fact Sheet No. 311*. March 2013.
2. Ramachandran, A. and C. Snehalatha, *Rising burden of obesity in Asia.* J Obes, 2010. **2010**: p. 1-8.
3. Jo, J.e.a., *Hypertrophy and/or hyperplasia: Dynamics of adipose tissue growth.* Plos Computational Biology, 2009. **5**(3): p. 1-11.
4. Sun, K.a.S., P.E., *Adipose tissue dysfunction: A multiple step process.* Novel Insights into Adipoce Cell Functions, 2010: p. 67-77.
5. Galic, S., J.S. Oakhill, and G.R. Steinberg, *Adipose tissue as an endocrine organ.* Mol Cell Endocrinol, 2010. **316**(2): p. 129-139.
6. Ferranti, D.e.a., *The perfect storm: obesity, adipocyte dysfunction, and metabolic consequences.* Clin Chem, 2008. **54**(6): p. 945-955.
7. Moreno-Navarrete, J.M.a.F.-R., J.M., *Adipocyte Differentiation.* 2012: p. 17-38.
8. Cristancho, A.G. and M.A. Lazar, *Forming functional fat: a growing understanding of adipocyte differentiation.* Nat Rev Mol Cell Biol, 2011. **12**(11): p. 722-734.
9. Evan D.Rosen, C.J.W., Pere Puigserver et al., *Transcriptional regulation of adipogenesis.* Genes Dev, 2000. **14**: p. 1293-1307.
10. Rosen, E.D.a.S., B.M, *Molecular regulation of adipogenesis.* Annu. Rev. Cell Dev. Biol., 2000. **16**: p. 145-152.
11. Tang, Q.Q., T.C. Otto, and M.D. Lane, *Mitotic clonal expansion: a synchronous process required for adipogenesis.* Proc Natl Acad Sci U S A, 2003. **100**(1): p. 44-49.

12. Tang, Q.Q., T.C. Otto, and M.D. Lane, *CCAAT/enhancer-binding protein beta is required for mitotic clonal expansion during adipogenesis.* Proc Natl Acad Sci U S A, 2003. **100**(3): p. 850-855.
13. Zhang, J.W., et al., *Dominant-negative C/EBP disrupts mitotic clonal expansion and differentiation of 3T3-L1 preadipocytes.* Proc Natl Acad Sci U S A, 2004. **101**(1): p. 43-47.
14. Sun, L., et al., *Long noncoding RNAs regulate adipogenesis.* Proc Natl Acad Sci U S A, 2013. **110**(9): p. 3387-3392.
15. Kim, J.E.a.C., J., *Regulation of PPARg activity by mammalian target of rapamycin and amino acids in adipopogenesis.* Diabetes, 2004. **53**: p. 2748-2757.
16. Rayalam, S., M.A. Della-Fera, and C.A. Baile, *Phytochemicals and regulation of the adipocyte life cycle.* J Nutr Biochem, 2008. **19**(11): p. 717-726.
17. Xu, J. and K. Liao, *Protein kinase B/AKT 1 plays a pivotal role in insulin-like growth factor-1 receptor signaling induced 3T3-L1 adipocyte differentiation.* J Biol Chem, 2004. **279**(34): p. 35914-35922.
18. Taniguchi, C.M., B. Emanuelli, and C.R. Kahn, *Critical nodes in signalling pathways: insights into insulin action.* Nat Rev Mol Cell Biol, 2006. **7**(2): p. 85-96.
19. Hiroshi Sakaue‡, W.O., Michihiro Matsumoto‡, Shoji Kuroda‡, Masafumi Takata‡,Tadanori Sugimoto‡, Bruce M. Spiegelman¶, and Masato Kasuga‡, *Posttranscriptional control of adipocyte differentiation through activation of Phosphoinositide 3-kinase.* The Journal of Biological Chemistry, 1998. **273**(44): p. 11.
20. Nogueira, V., et al., *Akt-dependent Skp2 mRNA translation is required for exiting contact inhibition, oncogenesis, and adipogenesis.* EMBO J, 2012. **31**(5): p. 1134-1146.

21. Qiu, Z., et al., *DNA synthesis and mitotic clonal expansion is not a required step for 3T3-L1 preadipocyte differentiation into adipocytes.* J Biol Chem, 2001. **276**(15): p. 11988-11995.
22. Aubin, D., A. Gagnon, and A. Sorisky, *Phosphoinositide 3-kinase is required for human adipocyte differentiation in culture.* Int J Obes (Lond), 2005. **29**(8): p. 1006-1009.
23. Tomiyama, K., et al., *Wortmannin, a specific phosphatidylinositol 3-kinase inhibitor, inhibits adipocytic differentiation of 3T3-L1 cells.* Biochem Biophys Res Commun, 1995. **212**(1): p. 263-269.
24. Adan, R.A., *Mechanisms underlying current and future anti-obesity drugs.* Trends Neurosci, 2013. **36**(2): p. 133-140.
25. Padwal, R.S. and S.R. Majumdar, *Drug treatments for obesity: orlistat, sibutramine, and rimonabant.* The Lancet, 2007. **369**(9555): p. 71-77.
26. Leiherer, A., A. Mundlein, and H. Drexel, *Phytochemicals and their impact on adipose tissue inflammation and diabetes.* Vascul Pharmacol, 2013. **58**(1-2): p. 3-20.
27. Kim, S.T., et al., *Hepatoprotective and antioxidant effects of Alnus japonica extracts on acetaminophen-induced hepatotoxicity in rats.* Phytother Res, 2004. **18**(12): p. 971-975.
28. Hu, W., et al., *The antidiabetic effects of an herbal formula composed of Alnus hirsuta, Rosa davurica, Acanthopanax senticosus and Panax schinseng in the streptozotocin-induced diabetic rats.* Nutr Res Pract, 2013. **7**(2): p. 103-108.
29. Lee, S.J., *Korea Folk Medicine.* Seoul National University Publishing Center Press, Seoul, 1996: p. 40.
30. Sati, S.C., N. Sati, and O.P. Sati, *Bioactive constituents and medicinal importance of genus Alnus.* Pharmacogn Rev, 2011. **5**(10): p. 174-183.
31. Lee, M., et al., *Anti-adipogenic diarylheptanoids from Alnus hirsuta f. sibirica on 3T3-L1 cells.* Bioorg Med Chem Lett, 2013. **23**(7): p. 2069-2073.

32. Nguyen Huu Tung1, S.K.K., Jeong Chan Ra2, Yu-Zhe and D.H.S. Zhao3, Young Ho Kim1, *Antioxidative and hepatoprotective diarylheptanoids from the bark of Alnus japonica.* Planta Med, 2010. **76**: p. 4.
33. Jeong, M.S., et al., *Atopic dermatitis-like skin lesions reduced by topical application and intraperitoneal injection of Hirsutenone in NC/Nga mice.* Clin Dev Immunol, 2010. **2010**: p. 1-7.
34. Kim, J.H., et al., *Hirsutenone inhibits phorbol ester-induced upregulation of COX-2 and MMP-9 in cultured human mammary epithelial cells: NF-kappaB as a potential molecular target.* FEBS Lett, 2006. **580**(2): p. 385-392.
35. Lee, C.S., et al., *Hirsutenone inhibits lipopolysaccharide-activated NF-kappaB-induced inflammatory mediator production by suppressing Toll-like receptor 4 and ERK activation.* Int Immunopharmacol, 2010. **10**(4): p. 520-525.
36. Lee, C.S., et al., *Diarylheptanoid hirsutenone enhances apoptotic effect of TRAIL on epithelial ovarian carcinoma cell lines via activation of death receptor and mitochondrial pathway.* Invest New Drugs, 2012. **30**(2): p. 548-557.
37. Kang, N.J., et al., *Cocoa procyanidins suppress transformation by inhibiting mitogen-activated protein kinase kinase.* J Biol Chem, 2008. **283**(30): p. 20664-73.
38. Kwon, J.Y., et al., *An inhibitory effect of resveratrol in the mitotic clonal expansion and insulin signaling pathway in the early phase of adipogenesis.* Nutr Res, 2012. **32**(8): p. 607-616.
39. Kwon, J.Y., et al., *Piceatannol, natural polyphenolic stilbene, inhibits adipogenesis via modulation of mitotic clonal expansion and insulin receptor-dependent insulin signaling in early phase of differentiation.* J Biol Chem, 2012. **287**(14): p. 11566-11578.
40. Bost, F., et al., *The role of MAPKs in adipocyte differentiation and obesity.* Biochimie, 2005. **87**(1): p. 51-6.

41. Fre´de´ ric Bost, M.A., Leslie Caron, Patrick Even, Nathalie Belmonte, Matthieu Prot,, P.H. Christian Dani, Gilles Page`s, Jacques Pouysse´gur, Yannick Le Marchand-Brustel,, and a.B. Bine´truy, *The extracellular signal-regulated kinase isoform ERK1 is specifically required for in vitro and in vivo adipogenesis.* Diabetes, 2005. **54**(2): p. 402-414.
42. Lee, S.J., et al., *A functional role for the p62-ERK1 axis in the control of energy homeostasis and adipogenesis.* EMBO Rep, 2010. **11**(3): p. 226-232.
43. Danesch, U., W. Hoeck, and G.M. Ringold, *Cloning and transcriptional regulation of a novel adipocyte-specific gene, FSP27. CAAT-enhancer-binding protein (C/EBP) and C/EBP-like proteins interact with sequences required for differentiation-dependent expression.* J Biol Chem, 1992. **267**(10): p. 7185-93.
44. Rosen, E.D., et al., *Transcriptional regulation of adipogenesis.* Genes Dev, 2000. **14**(11): p. 1293-1307.
45. Li, X., et al., *Role of cdk2 in the sequential phosphorylation/activation of C/EBPbeta during adipocyte differentiation.* Proc Natl Acad Sci U S A, 2007. **104**(28): p. 11597-11602.
46. Kim, C.Y., et al., *Curcumin inhibits adipocyte differentiation through modulation of mitotic clonal expansion.* J Nutr Biochem, 2011. **22**(10): p. 910-920.
47. Choi, K.M., et al., *Sulforaphane inhibits mitotic clonal expansion during adipogenesis through cell cycle arrest.* Obesity (Silver Spring), 2012. **20**(7): p. 1365-1371.
48. Ntambi, J.M. and K. Young-Cheul, *Adipocyte differentiation and gene expression.* J Nutr, 2000. **130**(12): p. 3122S-3126S.
49. Klemm, D.J., et al., *Insulin-induced adipocyte differentiation. Activation of CREB rescues adipogenesis from the arrest caused by inhibition of prenylation.* J Biol Chem, 2001. **276**(30): p. 28430-28435.

50. Bluher, M., et al., *Intrinsic heterogeneity in adipose tissue of fat-specific insulin receptor knock-out mice is associated with differences in patterns of gene expression.* J Biol Chem, 2004. **279**(30): p. 31891-31901.
51. Bluher, M., et al., *Adipose tissue selective insulin receptor knockout protects against obesity and obesity-related glucose intolerance.* Dev Cell, 2002. **3**(1): p. 25-38.
52. Helga M. L. Edelmann, C.K.h., Claudia Petritsch, and Lisa M. Ballou, *Cell cycle regulation of p70 S6 kinase and p42/p44 mitogen-activated protein kinases in Swiss Mouse 3T3-L1 fibroblasts.* The Journal of Biological Chemistry, 1996. **271**(2): p. 9.
53. Baudry, A., Z.Z. Yang, and B.A. Hemmings, *PKBalpha is required for adipose differentiation of mouse embryonic fibroblasts.* J Cell Sci, 2006. **119**(Pt 5): p. 889-897.
54. Zhang, H.H., et al., *Insulin stimulates adipogenesis through the Akt-TSC2-mTORC1 pathway.* PLoS One, 2009. **4**(e6189-6196): p. e6189.
55. Xia, X. and G. Serrero, *Inhibition of adipose differentiation by phosphatidylinositol 3-kinase inhibitors.* J Cell Physiol, 1999. **178**(1): p. 9-16.
56. Sale, E.M., Atkinson, P.G.P and Sale, G.J, *Requirement of MAP kinase for differentiationn of fibroblasts to adipocytes, for insulin activation of p90 S6 kinase and for insulin or serum stimulation of DNA synthesis.* The EMBO Journal, 1995. **14**(4): p. 674-684.
57. Claycombe, K.J., et al., *Insulin increases fatty acid synthase gene transcription in human adipocytes.* Am J Physiol, 1998. **274**(5 Pt 2): p. R1253-1259.
58. Liu, L.H., et al., *Effects of a fatty acid synthase inhibitor on adipocyte differentiation of mouse 3T3-L1 cells.* Acta Pharmacol Sin, 2004. **25**(8): p. 1052-1057.

59. Okada, T., et al., *Essential role of phosphatidylinositol 3-kinase in insulin-induced glucose transport and antilipolysis in rat adipocytes. Studies with a selective inhibitor wortmannin.* J Biol Chem, 1994. **269**(5): p. 3568-3573.
60. SHEPHERD P.R., N., B.T. and SIDDLE, K., *Insulin stimulation of glycogen synthesis and glycogen synthase activity is blocked by wortmannin and rapamycin in 3T3-L1 adipocytes: evidence for the involvement of phosphoinositide 3-kinase and p70 ribosomal protein-S6 kinase*. Biochemical Journal, 1995. **305**: p. 25-29.
61. Carvalho, E., C. Rondinone, and U. Smith, *Insulin resistance in fat cells from obese Zucker rats--evidence for an impaired activation and translocation of protein kinase B and glucose transporter 4.* Mol Cell Biochem, 2000. **206**(1-2): p. 7-16.
62. Taniguchi, C.M., et al., *Phosphoinositide 3-kinase regulatory subunit p85alpha suppresses insulin action via positive regulation of PTEN*. Proc Natl Acad Sci U S A, 2006. **103**(32): p. 12093-12097.

Figure 1

A

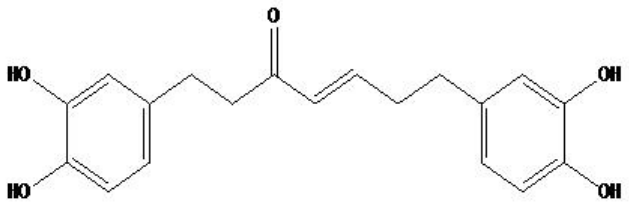

Hirsutenone (HST)

B

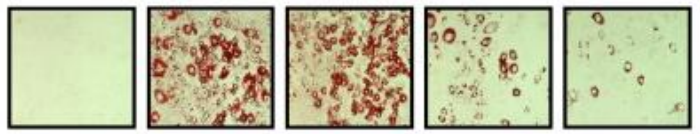

C

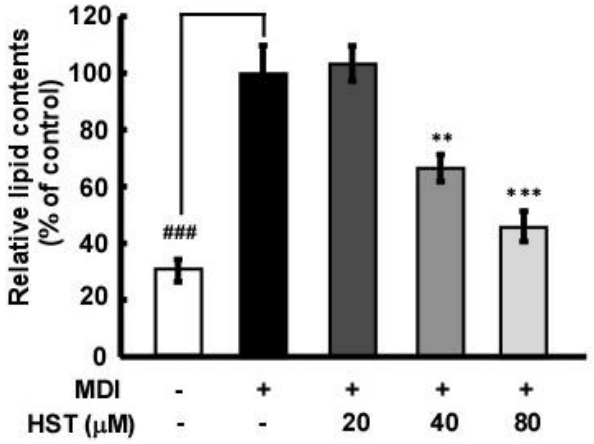
Relative lipid contents (% of control)
120
100
80
60
40
20
0
###
**
***
MDI - + + + +
HST (μM) - - 20 40 80

D

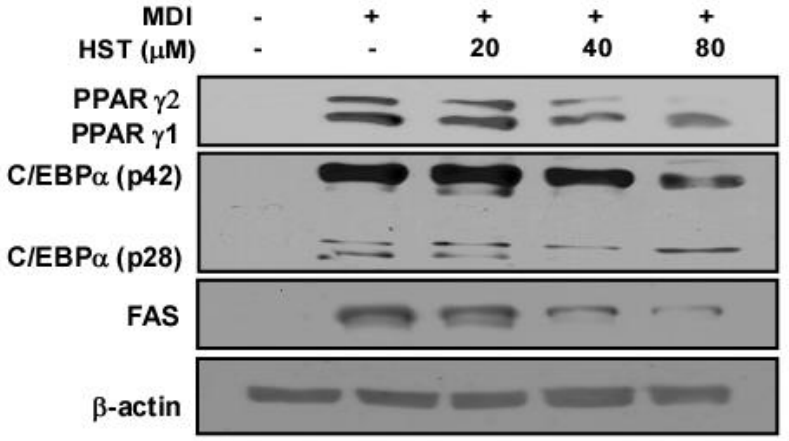
MDI - + + + +
HST (μM) - - 20 40 80
PPAR γ2
PPAR γ1
C/EBPα (p42)
C/EBPα (p28)
FAS
β-actin

E

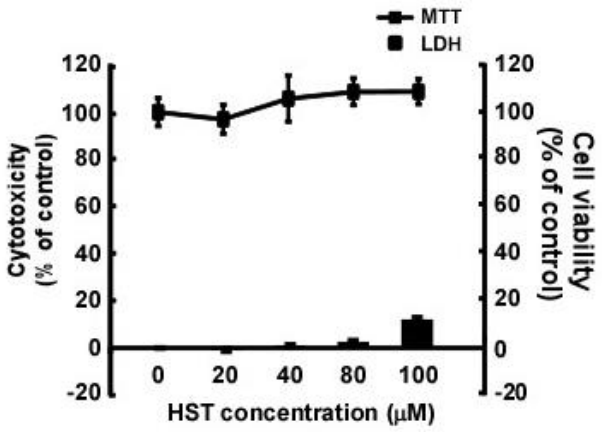
MTT
LDH
120
100
80
60
40
20
0
-20
Cytotoxicity
(% of control)
Cell viability
(% of control)
0
20
40
80
100
HST concentration (μM)

Figure 1. Hirsutenone inhibits adipogenesis in 3T3-L1 preadipocytes

(A) The chemical structure of hirsutenone (HST).

(B) Visualization of lipid accumulation by Oil Red O staining. Differentiation of 3T3-L1 preadipocytes were treated with HST at 20, 40 and 80 μM for 6 days.

(C) The Oil Red O stained lipid droplets in the differentiated cell were extracted with isopropanol for spectrometric quantification at 515 nm. Data are representative of 3 independent experiments that yielded similar results, which presented as means ± S.D. Significant difference between no differentiation group and MDI-treated group ($^{###}P < 0.001$). Significant difference between MDI-treated group and group treated with MDI and HST (**P < 0,01 and ***P < 0.001, respectively)

(D) Whole cell lysate was prepared to determine MDI-induced PPARγ, C/EBPα and FAS expression levels by western blot analysis after 6 days of differentiation.

(E) At post-confluence day, 3T3-L1 preadipocytes were incubated with DMEM supplemented with 10% FBS and MDI cocktail with various concentrations (20 – 100 μM) of HST for 2 days. The cytotoxicity and viability of cells were assessed by LDH and MTT assay, respectively. Cytotoxicity and cell viability was expressed as a percentage relative to control. Data are representative of 3 independent experiments that yielded similar results, which presented as means ± S.D.

Figure 2

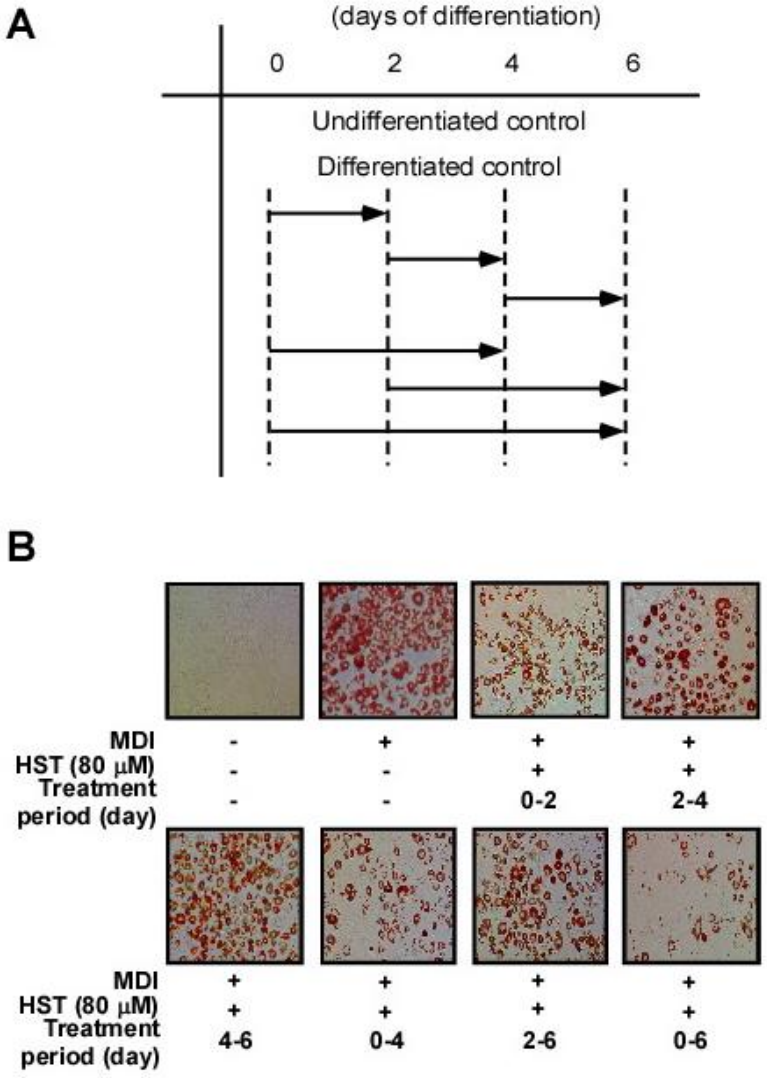
A
(days of differentiation)
0
2
4
6
Undifferentiated control
Differentiated control
B
MDI
HST (80 μM)
Treatment period (day)
- + + +
- - + +
- - 0-2 2-4
MDI
HST (80 μM)
Treatment period (day)
+ + + +
+ + + +
4-6 0-4 2-6 0-6

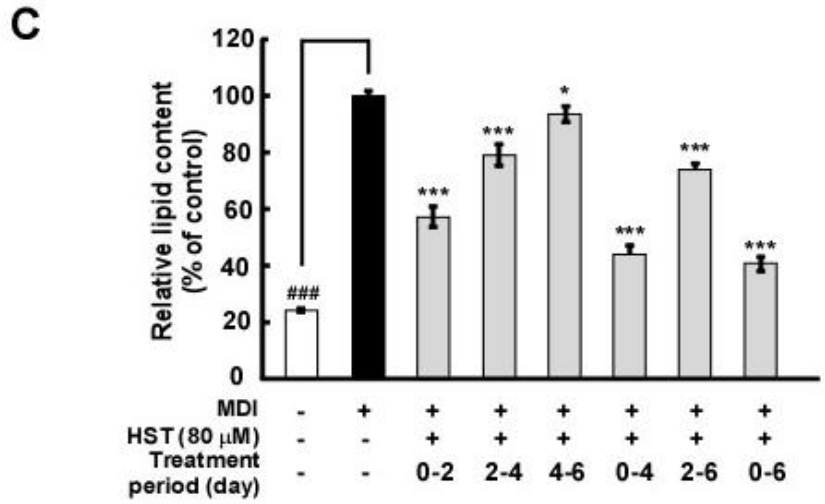

Figure 2. Effect of hirsutenone on MDI-induced differentiation of 3T3-L1 preadipocytes at different stages of adipogenesis

(A) A schematic diagram of 3T3-L1 cells were induced to differentiate with MDI. 80 μM HST was added in the indicated time period during adipogenesis. After 6 days of differentiation, adipocytes were subjected to Oil Red O (ORO) staining of intracellular lipids accumulation.

(B) Visualization of lipid accumulation from ORO-stained adipocytes.

(C) Spectrometric quantification of stained adipocytes at 515 nm. Relative lipid content was expressed as % compared to the control (only MDI-treated group). Data are representative of 3 independent experiments that yielded similar results, which presented as means ± S.D. independent experiments that yielded similar results, which presented as means ± S.D. Significant difference between no differentiation group and MDI-treated group ($^{###}P < 0.001$). Significant difference between MDI-treated group and group treated with MDI and HST ($^{*}P < 0.05$ and $^{***}P < 0.001$, respectively)

Figure 3

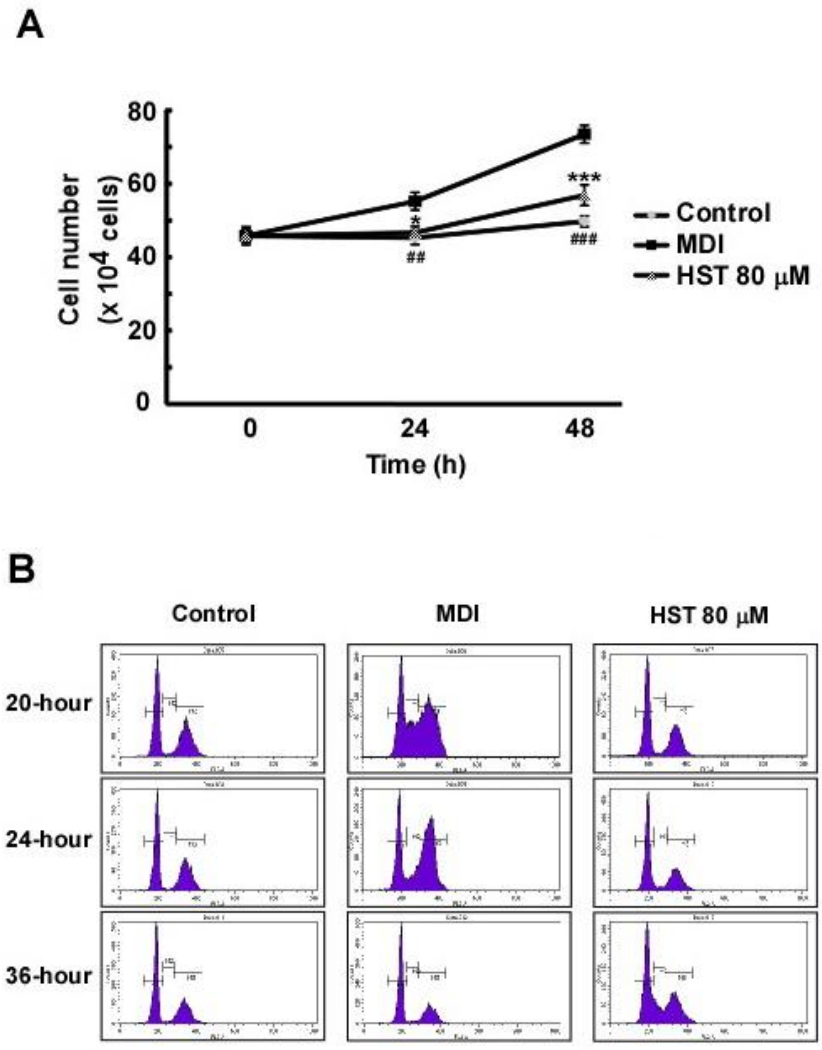
A
Cell number (x 10^4 cells)
80
60
40
20
0
0
24
48
Time (h)
***
*
##
###
Control
MDI
HST 80 μM
B
Control
MDI
HST 80 μM
20-hour
24-hour
36-hour

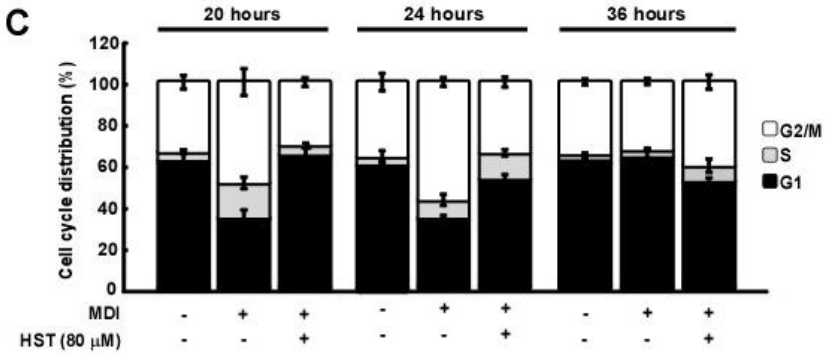
C
20 hours
24 hours
36 hours
Cell cycle distribution (%)
120
100
80
60
40
20
0
G2/M
S
G1
MDI
HST (80 μM)

Figure 3. Hirsutenone modulates MDI-induced MCE in the early stage of adipogenesis

Two days post-confluent 3T3-L1 preadipocytes were initiated to differentiate with MDI in the presence or absence of 80 μM HST The cells were harvested at the indicated time and stained with propidium iodide for flow cytometer cell cycle analysis.

(A) The effects of hirsutenone on MDI-induced cell proliferation was evaluated by Trypan blue assay.

(B) The histogram result indicated cell cycle distribution in G1, S or G2/M phases after treating with 80 μM HST.

(C) Quantitative data is presented in bar graph for 20 hours, 24 hours and 36 hours. Data are representative of 3 independent experiments with similar results which presented as means ± S.E.

Figure 4

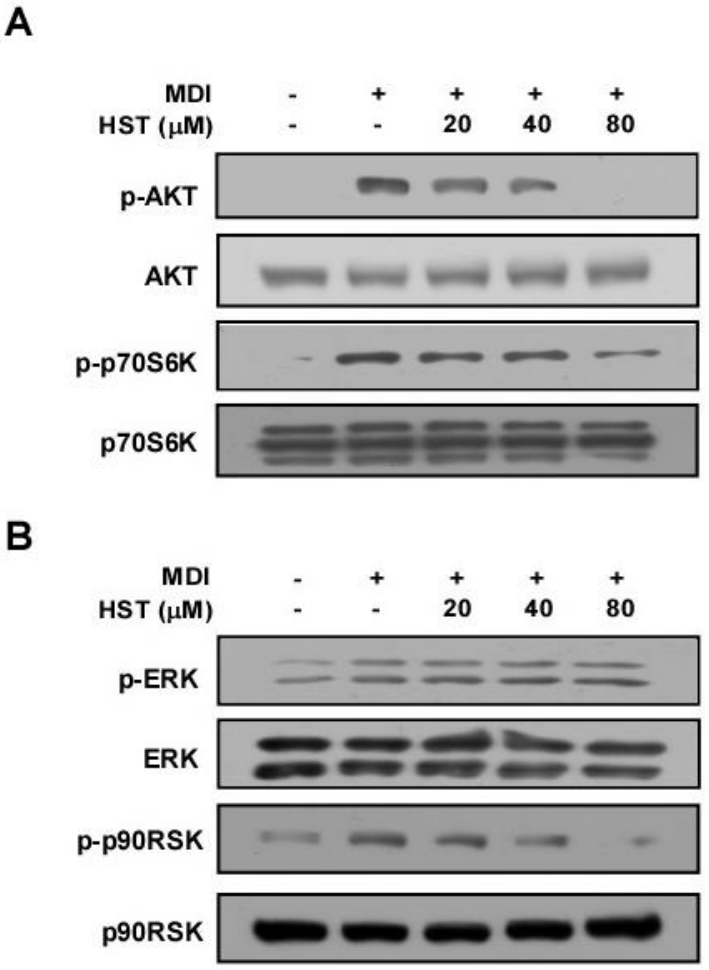
A
MDI - + + + +
HST (μM) - - 20 40 80
p-AKT
AKT
p-p70S6K
p70S6K
B
MDI - + + + +
HST (μM) - - 20 40 80
p-ERK
ERK
p-p90RSK
p90RSK

Figure 4. Inhibitory effect of hirsutenone on MDI-induced Akt and ERK-mediated signaling pathway in the early s of adipogenesis

(A) Phosphorylation of Akt (Ser 473) and p70S6K in differentiating cells treated with 20, 40 and 80 μM HST for 1 hour were measured by western blot analysis.

(B) Phosphorylated ERK and p90RSK were analyzed by western blot analysis after 15 minutes treatment of 20, 40 and 80 μM HST.

All data are representative of 3 independent experiments that yielded similar results.

Figure 5

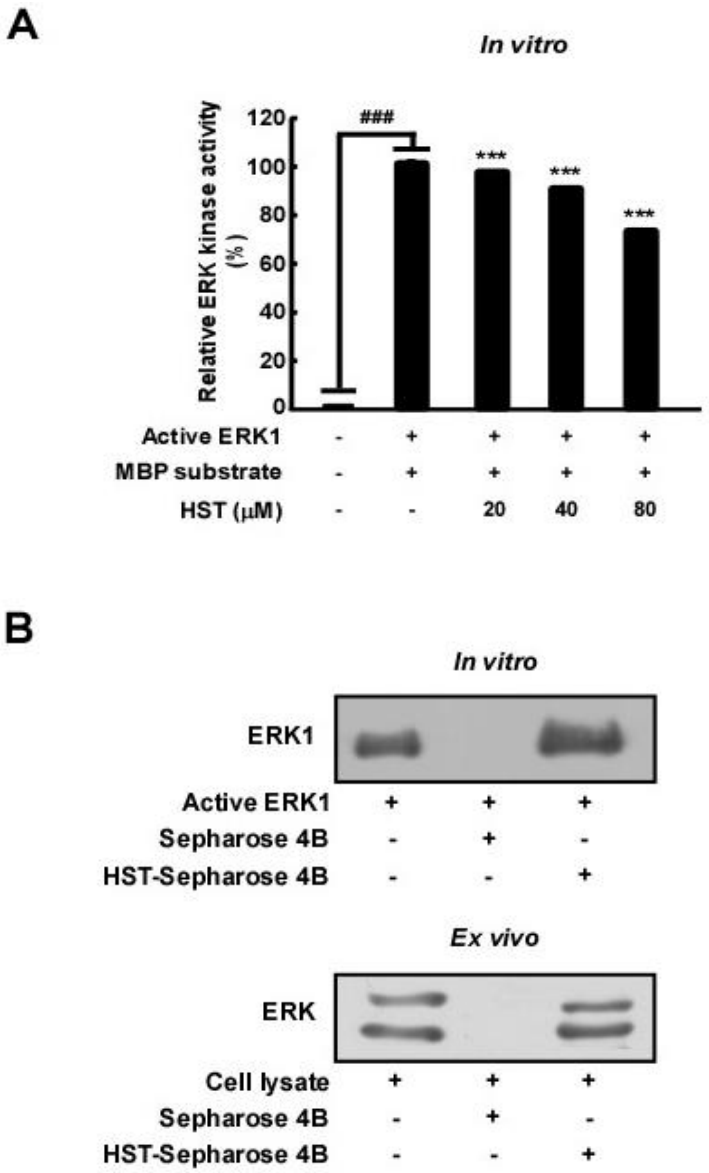
A
In vitro
Relative ERK kinase activity (%)
120
100
80
60
40
20
0
###
***
***
***
Active ERK1 - + + + +
MBP substrate - + + + +
HST (μM) - - 20 40 80
B
In vitro
ERK1
Active ERK1 + + +
Sepharose 4B - + -
HST-Sepharose 4B - - +
Ex vivo
ERK
Cell lysate + + +
Sepharose 4B - + -
HST-Sepharose 4B - - +

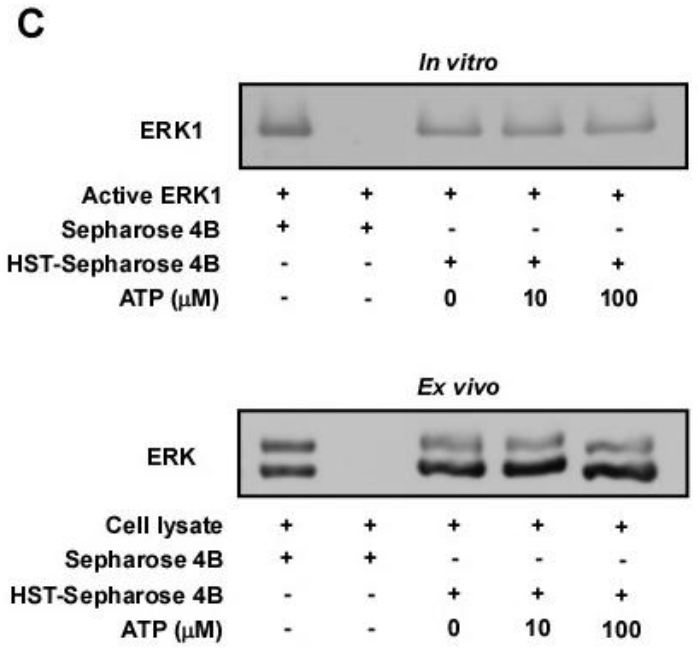

Figure 5. Inhibitory effect of hirsutenone on ERK1 activity

(A) *In vitro* ERK1 activity was analyzed in the presence or absence of HST (20, 40 and 80 μM). Kinase activity is expressed as count per minute (cpm).

(B) *In vitro* and *ex vivo* binding of HST with ERK1 was performed by pull down assay.

(C) *In vitro* and *ex vivo* ATP competitive assay was performed to determine whether HST binds with ERK1 in an ATP-competitive manner.

All data above are representative of 3 independent experiments that yielded similar results which presented as means ± S.D. ($^{###}P < 0.001$). Significant difference between absence and presence of HST-treated groups (***$P < 0.001$).

Figure 6

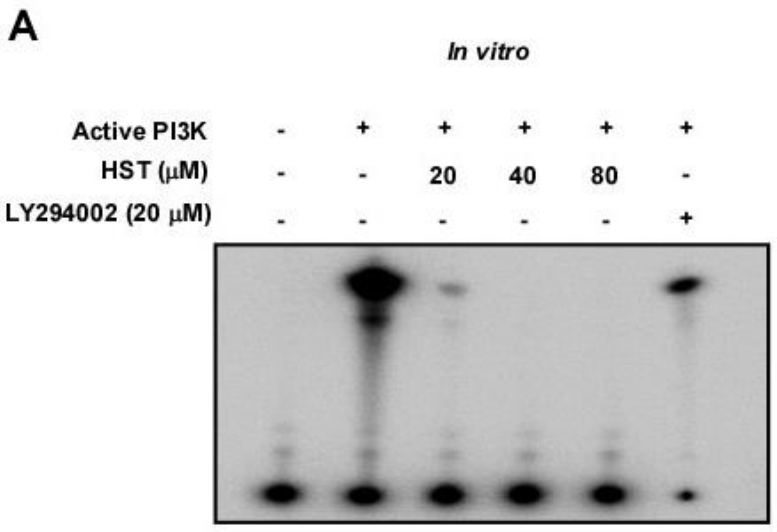
A
In vitro
Active PI3K - + + + + +
HST (μM) - - 20 40 80 -
LY294002 (20 μM) - - - - - +

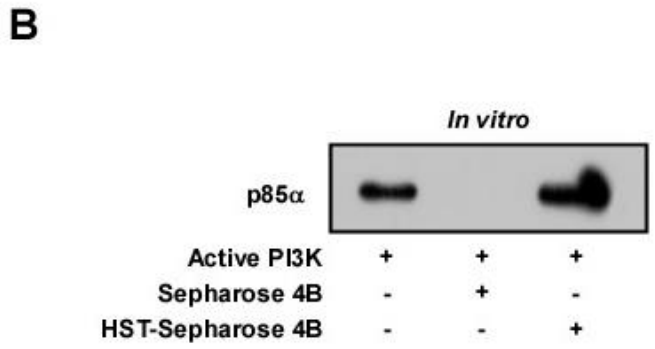
B
In vitro
p85α
Active PI3K + + +
Sepharose 4B - + -
HST-Sepharose 4B - - +

Figure 6. Inhibitory effect of hirsutenone on PI3K activity

(A) *In vitro* PI3K activity was analyzed in the presence or absence of HST (20, 40 and 80 μM) or 20 μM LY294002. The ^{32}P-labeled phosphatidylinositol-3-phosphate product was resolved through thin layer chromatography and visualized by autoradiography.

(B) *In vitro* binding of HST with PI3K protein was performed by pull down assay.

Figure 7

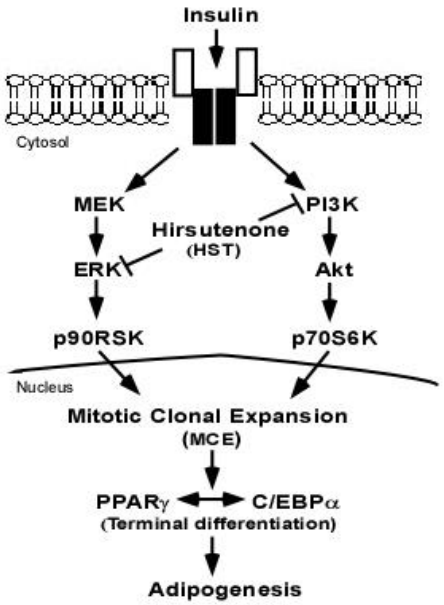

Figure 7. Proposed depiction of the anti-adipogenic mechanism of hirsutenone in 3T3-L1 preadipocytes

VI. 국문초록

과체중과 비만의 비약적인 증가는 세계적인 건강 문제로 대두되어 왔다. 비만치료제의 부작용 때문에 비만을 예방하거나 치료하기 위한 많은 가능성 있는 천연 물질들이 대체제로 개발되고 있다. 본 석사학위 청구논문에서는 diarylheptanoid 구조인 허수테논 (hirsutenone)을 이용하여 3T3-L1 지방전구세포의 분화 억제능을 밝히고, 관련 메커니즘 규명 및 분자 표적 발굴에 관한 연구를 수행하였다. 허수테논은 분화유도혼합물에 의해 유도되는 지질 축적을 지방세포분화의 주요 조절 마커인 PPARγ, C/EBPα, FAS 발현을 감소시킴으로써 농도의존적으로 억제하였다. 허수테논의 지방세포분화 억제 효능은 지방세포 분화의 초기 단계인

유사분열성 세포증식 (mitotic clonal expansion, MCE) 의 G1 에서 S 단계로의 진입 지연에 의해 주로 일어났다. 허수테논의 유사분열성 세포증식 억제는 주로 두 타겟을 통하여 이루어졌다. 첫 번째는 인슐린 신호에 의해 활성화되는 PI3K 의 활성을 효과적으로 억제함으로써 그 하위 조절자인 Akt 의 인산화를 억제하여 이루어졌다. 두 번째는 ERK 의 활성을 저해함으로써 그 하위 기질인 p90RSK 의 인산화를 억제하여 이루어짐을 관찰하였다. 결과적으로, 본 연구에서는 허수테논이 PI3K 와 ERK 의 활성을 억제함으로써 지방세포형성 초기단계인 유사분열성 세포증식을 조절하여 3T3-L1의 지방세포분화형성을 억제함을 밝혔다.

주요어 : 허수테논; 지방세포분화형성; 유사분열성 세포증식; PI3K; ERK; 3T3-L1 지방전구세포

학 번 : 2011-24270